



ELSEVIER

Homogeneous hydrogenation of diphenylacetylene in the presence of $\text{Ru}_3(\text{CO})_9\text{L}_3$ ($\text{L} = \text{PPh}_3$, PEt_3). The crystal structure of $\text{Ru}_3(\text{CO})_{10}(\text{PEt}_3)_2$: a reaction intermediate?

Giuliana Gervasio ^{a,*}, Roberto Giordano ^a, Domenica Marabello ^a, Enrico Sappa ^b

^a *Dipartimento di Chimica IFM, Università di Torino, Via Pietro Giuria 7, I-10125 Turin, Italy*

^b *Dipartimento di Scienze e Tecnologie Avanzate, Università del Piemonte Orientale Amedeo Avogadro, Corso Borsalino 54, I-15100 Alessandria, Italy*

Received 8 April 1999

Abstract

The phosphine-substituted clusters $\text{Ru}_3(\text{CO})_9\text{L}_3$ ($\text{L} = \text{PPh}_3$, **1**; $\text{L} = \text{PEt}_3$, **2**) are active homogeneous catalysts for the hydrogenation of diphenylacetylene. In the catalytic reactions involving complex **2**, formation of $\text{Ru}_3(\text{CO})_{10}(\text{PEt}_3)_2$ (**3**) has been observed. This complex shows a hydrogenating activity greater than that of the parent complex **2**. In the light of these results and of the observed effect of dihydrogen pressure and substrate/cluster ratio, reaction mechanisms are discussed. The structure of **3** has been characterized by X-ray diffraction and is compared with those of other phosphine-substituted triruthenium clusters. Compound **3** crystallizes in the monoclinic space group $P2_1$ with $a = 9.368(7)$, $b = 12.20(2)$, $c = 13.554(9)$ Å, $\beta = 102.63(8)^\circ$ and $Z = 2$. Refinement of 4975 data gave $R_1 = 0.0417$ and $wR_2 = 0.1105$. The two phosphorus ligands occupy equatorial positions on adjacent metal atoms so that they are *trans* to each other at the ends of the Ru–Ru vector. The presence of bent semi-bridging carbonyl groups makes the molecule chiral and its absolute structure was determined. © 1999 Elsevier Science S.A. All rights reserved.

Keywords: Homogeneous catalysis; Hydrogenation; Phosphine-substituted ruthenium clusters; Reaction intermediates; X-ray absolute structure

1. Introduction

Homo- and heterometallic ruthenium-containing carbonyl clusters catalyze the hydrogenation of alkynes [1] and of cyclic dienes [2]. For some of these reactions structure–reactivity relationships have been observed [3] and reaction intermediates or byproducts have been isolated and characterized [1–4]. In some instances, reaction mechanisms based on the nature of the above derivatives have been proposed [3b].

We had already observed that the substitution of phosphine ligands for carbonyls may increase the catalytic activity: this occurred, for example, in the hydrogenation–isomerization reactions of linear dienes in the presence of complexes $\text{Ru}_3(\text{CO})_9(\text{PPh}_3)_3$ (**1**) and $\text{Ru}_3(\text{CO})_9(\text{PEt}_3)_3$ (**2**) [5]. We found that the presence of CO did not inhibit these reactions, although it usually

did. Clusters **1** and **2**, however, had not been tested as hydrogenation catalysts for alkynes; therefore the comparison with the activity of other ruthenium-based substituted and unsubstituted derivatives that have been the object of recent studies [1–4] was so far not possible.

Here we report on the behavior of complexes **1** and **2** as homogeneous catalysts for the hydrogenation of C_2Ph_2 . We find that the above clusters show a considerable catalytic activity. In particular, under the thermal conditions adopted, cluster **2** gives rise to complex **3**, which in turn is considerably active in hydrogenation. This behaviour is discussed.

The structure of **3** has been determined by X-ray diffraction and is compared with those of other tri- and bi-substituted triruthenium derivatives. In principle cluster bonding parameters should depend on the electron-donor ability as well as on the steric hindrance of the phosphine ligands. The catalytic behavior of the substituted clusters should also be related to the elec-

* Corresponding author.

E-mail address: gervasio@silver.ch.unito.it (G. Gervasio)

tronic effects of the ligands. By contrast, during this study we have found that catalytic activity is mainly influenced by the chemical reactivity of clusters (e.g. tendency to fragmentation and/or disproportionation); this kind of reactivity, however, cannot be directly related to the observed structural parameters.

2. Experimental

2.1. Synthesis of complexes **1** and **2**

The syntheses of complexes **1** and **2** have already been described [6]. Complex **1** was obtained by refluxing for 1 min $\text{Ru}_3(\text{CO})_{12}$ with a 1.5/1 M excess of triphenylphosphine in hexane under N_2 in the presence of Me_3NO . A deep red solution (and a violet insoluble residue) was obtained, which, after thin-layer chromatography (TLC) separation, gave some unreacted parent cluster, $\text{Ru}_3(\text{CO})_{11}(\text{PPh}_3)$ (ca. 10%), $\text{Ru}_3(\text{CO})_{10}(\text{PPh}_3)_2$ (ca. 50%) and complex **1** (ca. 30%). IR (C_6H_{14}): 2046 s, 1980 vs, 1967 vs, cm^{-1} . ^{31}P -NMR: + 31.3 s.

Complex **2** was obtained by refluxing for 30 s in hexane under N_2 $\text{Ru}_3(\text{CO})_{12}$ with an excess of PET_3 and Me_3NO . TLC of the clear, red solution, yielded 75% of **2** slightly contaminated by **3** (see below) and about 15% of an unidentified yellow product, together with some decomposition. IR (C_6H_{14}): 2061 s*, 2016 w, 1986 s, 1968 s, 1947 vs, cm^{-1} . ^{31}P -NMR: + 11.71 s*, + 32.69 s. (The signals marked with * are presumably due to impurities, e.g. complex **3**).

2.2. Homogeneous catalytic reactions

Catalytic reactions were performed, as previously described [1,2], in 25 ml sealed glass vials each containing 2 ml of an *n*-octane solution of the complex and diphenylacetylene under the appropriate pressure of dihydrogen. The vials were sealed and then warmed in an oven at 120°C for the required reaction time. Details of the reagent concentration and of the reaction conditions are given as footnotes to Table 1.

The organic products in the reaction solutions were analyzed with a Carlo Erba FID 4200 gas chromatograph equipped with a (2 m × 0.6 mm i.d.) SE 30 5% on Chromosorb WAW (60/80 mesh) column operated under the following conditions: N_2 flow 46 ml min^{-1} , 60°C (6 min) then 10°C min^{-1} up to 240°C.

The reaction solutions were analyzed by means of IR spectroscopy (Bruker Equinox 55, KBr cells) then chromatographed on TLC preparative plates on which the organometallic products were separated. These were analyzed by IR spectroscopy.

2.3. Identification of the organometallic products in the reaction solutions

All the (clear) solutions of the catalytic experiments involving cluster **1** changed over time from red to pale yellow. IR spectra showed the presence of some unaltered **1** together with bands at 2060, 2029, 2011 and 1960 cm^{-1} that could belong to (not isolated) $\text{Ru}_3(\text{CO})_{10}(\text{PPh}_3)_2$; in the experiment under CO/H_2 these signals were more intense.

All the solutions of the catalytic experiments with cluster **2** changed from dark orange to pale yellow; after the experiments under 1 atm of H_2 , with decreasing amounts of dihydrogen or by changing substrate/cluster (S/C) ratios, IR spectra showed the presence of unaltered cluster **2** together with cluster **3** in nearly equal amounts. After the experiments under CO/H_2 , however, only weak signals for cluster **2** and no signals for **3** were observed.

The solutions of the experiments involving cluster **3** turned from dark orange to yellow; the change in colour was slow when CO/H_2 was used. IR spectra showed the presence of unaltered complex **3** and some complex **2**, together with bands attributable to unidentified (mononuclear?) complexes.

2.4. Independent synthesis of complex **3**

A sample of complex **2** was heated at reflux in hexane under N_2 for 3–5 min. The red colour of the solution remained unaltered. TLC separation showed the presence of the unreacted parent complex (about 20%), complex **3** (about 60%) and some unidentified yellow products. IR (C_6H_{14}): 2061 vs, 2011 vs, 2001 vs, 1966 m, cm^{-1} . ^{31}P -NMR: + 11.71 s. This complex was crystallized from hexane for X-ray analysis and for catalytic experiments. Satisfactory elemental analyses were obtained for **3** as well as for **1** and **2**.

2.5. X-ray analysis of complex **3**

The data were collected at room temperature on a Siemens P4 diffractometer using graphite monochromatized Mo-K_α radiation. Three standard reflections measured every 50 reflections showed no decay. Cell constants were obtained from least-squares refinement based on the setting angles of 26 reflections in the range $20^\circ < 2\theta < 35^\circ$. Empirical absorption correction was performed according to the method of reference [7].

The structure was solved by direct methods and refined using the programs SHELXS-86 and SHELXL-93 (PC version), respectively. The absolute structure was determined using the Flack parameter (Table 2) [8]. Crystal data and refinement parameters are reported in Table 2.

Table 1
Hydrogenation of diphenylacetylene in the presence of clusters 1–3^a

Experiment	Reaction time (min)	Conversion	TON	Selectivity		
				<i>cis</i> -SB	<i>trans</i> -SB	C ₂ Ph ₂ H ₄
<i>Cluster 1</i>						
A	15	9.0	68.6	33.7	41.4	24.9
	30	25.3	192.9	57.7	33.9	8.4
	45	15.4	116.9	60.2	32.8	7.0
B	30	12.9	98.5	57.9	34.2	7.9
	30	5.5	41.9	28.0	52.6	19.3
	30	4.9	37.2	31.2	54.0	14.8
C'	30	17.7	205.4	40.5	54.4	5.1
	30	25.0	140.8	40.3	54.1	5.5
	30	28.3	82.8	40.3	54.1	5.6
C''	30	30.1	56.7	40.8	50.5	8.7
	30	24.7	93.0	48.3	43.4	8.3
	30	18.1	136.3	56.6	35.3	8.1
D	15	7.0	26.8	43.2	37.7	19.1
	30	8.2	31.1	61.1	22.7	16.2
	45	5.0	19.1	51.4	27.1	21.5
<i>Cluster 2</i>						
E	15	10.9	16.7	53.8	36.7	9.4
	30	63.7	97.7	59.1	40.2	0.6
	45	58.5	89.6	51.2	48.1	0.7
F	30	67.0	103.9	52.7	46.2	1.1
	30	36.4	56.4	55.9	43.5	0.5
	30	1.6	2.4	27.6	62.2	10.3
G'	30	42.9	72.9	53.6	45.3	1.0
	30	80.6	69.9	50.3	49.2	0.5
	30	99.4	50.6	14.1	85.0	0.8
G''	30	93.5	119.2	55.7	43.5	0.8
	30	79.2	202.0	61.5	37.9	0.6
	30	56.7	289.2	65.4	34.0	0.6
H	15	12.1	20.6	88.6	9.9	1.5
	30	16.2	27.6	86.4	12.5	1.0
	45	21.1	35.9	87.9	11.3	0.8
<i>Cluster 3</i>						
J	15	3.3	9.3	50.4	37.6	11.9
	30	42.0	117.2	55.6	43.6	0.8
	45	52.1	145.4	62.5	37.1	0.4
K	30	51.4	143.4	57.3	42.2	0.5
	30	27.1	75.7	54.6	44.1	1.2
	30	21.7	60.6	54.1	43.9	2.0
I'	30	37.3	57.2	54.1	44.7	1.1
	30	69.8	56.6	56.1	42.6	1.3
	30	98.6	36.4	46.6	52.2	1.2
I''	30	89.1	102.4	55.4	43.2	1.4
	30	68.5	157.5	58.3	40.5	1.2
	30	41.8	192.2	64.8	34.3	0.9
L	15	11.5	17.7	87.9	8.4	3.7
	30	21.7	33.6	91.2	7.1	1.7
	45	27.9	43.1	91.7	7.0	1.2

^a Experimental conditions: *t* always 120°C. (A) Substrate/cluster (S/C) = 761.1, H₂ = 1 atm. (B) S/C = 763.8, H₂ = 1.0, 0.5, 0.25 atm. (C') S/C = 1158.3, 563.1, 292.6, H₂ = 1 atm. (C'') S/C = 188.3, 376.5, 753.0, H₂ = 1 atm. (D) S/C = 381.2, CO/H₂ 50/50 (0.5/0.5 atm). (E) S/C = 153.3, H₂ = 1 atm. (F) S/C = 154.9, H₂ = 1.0, 0.5, 0.25 atm. (G') S/C = 170.0, 86.7, 50.9, H₂ = 1 atm. (G'') S/C = 127.5, 255.0, 510.0, H₂ = 1 atm. (H) S/C = 170.0, H₂/CO 50/50. (J) S/C = 278.9, H₂ = 1 atm. (K) S/C = 278.9, H₂ = 1.0, 0.50, 0.25 atm. (I') S/C = 153.3, 81.1, 36.9, H₂ = 1 atm. (I'') S/C = 115.0, 229.9, 459.8, H₂ = 1 atm. (L) S/C = 154.4, H₂/CO 50/50.

Table 2
Crystal data and structure refinement parameters for $\text{Ru}_3(\text{CO})_{10}(\text{PEt}_3)_2$ (complex **3**)

Identification code	Complex 3
Empirical formula	$\text{C}_{22}\text{H}_{30}\text{O}_{10}\text{P}_2\text{Ru}_3$
Formula weight	819.61
Temperature (K)	293(2) K
Wavelength (Mo–K α) (Å)	0.71073
Crystal system	Monoclinic
Space group	$P2_1$
Unit cell dimensions	
a (Å)	9.368(7)
b (Å)	12.20(2)
c (Å)	13.554(9)
β (°)	102.63(8)
V (Å ³)	1511(2)
Z	2
D_{calc} (g cm ⁻³)	1.801
Absorption coefficient (mm ⁻¹)	1.632
$F(000)$	808
Crystal size (mm)	$0.30 \times 0.42 \times 0.48$
Color	Black
θ range for data collection (°)	1.54–31.41
Scan type	ω
Scan speed (° min ⁻¹)	Variable; 4.00–20.00
Scan range (°)	1.6
Standard reflections	3 measured every 50 reflections
Limiting indices	$-1 \leq h \leq 13$, $-1 \leq k \leq 17$, $-19 \leq l \leq 18$
Reflections collected	5823
Independent reflections	4975 [$R_{\text{int}} = 0.0385$]
Absorption correction	Semi-empirical from psi-scans
Max. and min. transmission	0.258 and 0.178
Refinement method	Full-matrix least-squares on F^2
Data/restraints/parameters	4975/1/336
Goodness-of-fit on F^2 ^a	0.977
Final R indices [4492 data with $I > 2\sigma(I)$]	$^b R_1 = 0.0353$, $^c wR_2 = 0.0988$
R indices (all data)	$^b R_1 = 0.0417$, $^c wR_2 = 0.1105$
Absolute structure parameter	-0.04(5)
Extinction coefficient	0.0111(7)
Largest diff. peak and hole (e Å ⁻³)	0.779 and -0.941

^a Goodness-of-fit = $[\sum[w(F_o^2 - F_c^2)^2]/(n-p)]^{1/2}$.

^b $R_1 = \sum||F_o| - |F_c||/\sum|F_o|$.

^c $wR_2 = [\sum[w(F_o^2 - F_c^2)^2]/(\sum(F_o^2)^2)]^{1/2}$.

All non-hydrogen atoms were anisotropically refined. The H atoms of the triethylphosphine ligands were calculated and refined riding on the corresponding carbon atoms with the isotropic temperature factors fixed at $1.2U_{\text{eq}}$ of the carbon atoms to which they are linked.

Table 3 lists atomic coordinates and equivalent isotropic displacement parameters for all non-hydrogen atoms, with the corresponding estimated S.D.s in parentheses.

3. Results and discussion

3.1. Hydrogenation reactions

The results of the hydrogenation experiments are collected in Table 1. The observed order of activity is $\text{Ru}_3(\text{CO})_9(\text{PPh}_3)_3$ (**1**) > $(\text{Ru}_3(\text{CO})_{10}(\text{PEt}_3)_2$ (**3**) > $(\text{Ru}_3(\text{CO})_9(\text{PEt}_3)_3$ (**2**). This behavior could point to the possibility that the electron-donor ability of the phosphine ligands plays a role in affecting catalytic activities. For example, the electron-withdrawing PPh_3 would weaken the cluster frame and favor fragment catalysis, whereas the electron-donating PEt_3 would strengthen the cluster and favor cluster catalysis. Indeed, fragment catalysis (as discussed below) would explain the observed lower activity of **3** with respect to **1**.

Table 3

Atomic coordinates ($\times 10^4$) and equivalent isotropic displacement parameters ($\text{Å}^2 \times 10^3$) for $\text{Ru}_3(\text{CO})_{10}(\text{PEt}_3)_2$ (complex **3**)^a

	x	y	z	U_{eq}
Ru(1)	-7085(1)	-4271(1)	-3224(1)	41(1)
Ru(2)	-6399(1)	-3963(1)	-1074(1)	47(1)
Ru(3)	-8313(1)	-2467(1)	-2353(1)	43(1)
P(1)	-5708(2)	-5739(2)	-3632(1)	45(1)
C(1)	-3863(8)	-5903(8)	-2862(6)	57(2)
C(2)	-2899(10)	-6790(11)	-3202(9)	81(3)
C(3)	-6505(9)	-7107(7)	-3559(7)	62(2)
C(4)	-7881(10)	-7319(10)	-4388(9)	86(3)
C(5)	-5404(9)	-5706(8)	-4931(6)	62(2)
C(6)	-4606(12)	-4735(10)	-5204(7)	81(3)
P(2)	-9586(2)	-1177(2)	-1576(1)	49(1)
C(7)	-10262(11)	-1594(8)	-448(7)	69(2)
C(8)	-9093(15)	-1735(12)	491(7)	94(4)
C(9)	-11318(10)	-773(10)	-2461(7)	72(2)
C(10)	-12200(12)	113(12)	-2118(10)	101(4)
C(11a)	-8670(11)	110(8)	-1197(8)	73(2)
C(12a)	-8333(14)	785(11)	-2045(11)	101(4)
C(11)	-8117(8)	-4044(8)	-4572(5)	56(2)
O(11)	-8732(8)	-3906(9)	-5378(5)	93(3)
C(12)	-5534(8)	-3218(6)	-3293(5)	49(2)
O(12)	-4633(7)	-2646(6)	-3362(5)	70(2)
C(13)	-8506(8)	-5273(7)	-2859(6)	55(2)
O(13)	-9330(7)	-5868(7)	-2691(6)	85(2)
C(21)	-6304(9)	-5508(9)	-911(6)	61(2)
O(21)	-6287(11)	-6423(7)	-771(7)	98(3)
C(22)	-4384(9)	-3698(9)	-1220(6)	62(2)
O(22)	-3194(7)	-3542(9)	-1209(6)	94(3)
C(23)	-5919(9)	-3529(8)	320(5)	57(2)
O(23)	-5590(8)	-3344(8)	1165(4)	82(2)
C(24)	-8512(8)	-3903(8)	-1090(5)	55(2)
O(24)	-9556(6)	-4160(6)	-826(4)	67(2)
C(31)	-8420(8)	-1660(7)	-3555(6)	55(2)
O(31)	-8478(9)	-1180(8)	-4297(5)	90(2)
C(32)	-6425(8)	-1817(9)	-1728(7)	64(2)
O(32)	-5457(7)	-1255(7)	-1481(6)	82(2)
C(33)	-10134(7)	-3239(7)	-2905(5)	50(2)
O(33)	-11237(6)	-3618(7)	-3207(5)	76(2)

^a U_{eq} is defined as one third of the trace of the orthogonalized U_{ij} tensor.

In the experiments under 1 atm of dihydrogen, a regular increase of the turnover numbers (TONs) with time is observed, except for cluster **1** that gives a maximum after 30 min, then a decrease. In all experiments an increase in the amount of *cis*-stilbene is also observed; this is particularly evident for cluster **1**. A decrease of dihydrogen pressure results in a gradual decrease of TON for all of the clusters; a decrease of the amount of *cis*-stilbene and an increase of the fully hydrogenated product is also observed.

In the experiments performed varying the amount of C_2Ph_2 , a decrease of the S/C ratio results in a regular decrease of TON for all of the clusters suggesting fragment catalysis; however, for **1** and **3** the *cis/trans*-stilbene ratio remains constant or changes only very little, whereas for **2** a sharp decrease in the amount of *cis*-stilbene is observed. Moreover, in the experiments performed varying the amount of the clusters, the TON increases as the metal concentration decreases, pointing to the possibility that all of the clusters examined fragment partially to mononuclear species and/or smaller clusters and that some or all of the species become catalytically active. Finally, the use of CO results in lower catalytic activities for all of the clusters; this could also be due, in part, to the lower pressure of dihydrogen present (H_2/CO 50:50). However, increasing TONs with time were observed in the experiments involving cluster **2** as well as cluster **3**. This behavior could suggest that CO favors dismutation and formation of active precursors. Formation of mononuclear fragments (active in isomerization) would be instead disfavored; this would be accounted for by the strong decrease of *trans*-stilbene when CO is used.

3.2. Formation of complex **3**

It is known that $Ru_3(CO)_{12-n}L_n$ complexes undergo thermal 'disproportionation' reactions under conditions comparable with those adopted in this work. Favored final products are $Ru_3(CO)_{10}L_2$ derivatives, closely related to complex **3**. Two hypotheses have been set forth about these reaction mechanisms; one consists in inter- or intramolecular phosphine exchange [9], but kinetic studies indicate that fragmentation does occur and that there is an equilibrium between mono-, bi- and trinuclear fragments or complexes [10].

3.3. Structure of complex **3** — a comparison with other phosphine-substituted ruthenium complexes

The structure of complex **3** is shown in Fig. 1 and relevant distances and angles are reported in Table 4. The molecular structure of complex **3** consists of a triangle of Ru atoms, with the two phosphine ligands equatorially bonded to two different Ru atoms in approximately *trans* configuration (type 1, Table 6). The

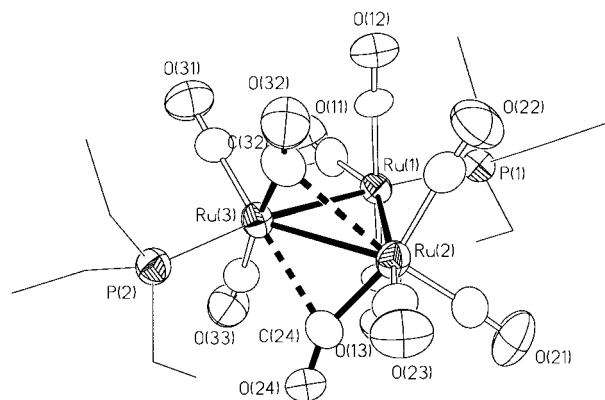


Fig. 1. An ORTEP plot (30% probability ellipsoids) of the molecular structure for complex $Ru_3(CO)_{10}(PEt_3)_2$ (**3**). Hydrogen atoms and selected labels have been omitted for clarity.

carbonyl ligands positions are distorted with respect to those observed in the parent complex $Ru_3(CO)_{12}$ [11]. In fact only the ligands on Ru(1) maintain the equatorial and axial positions found in $Ru_3(CO)_{12}$, while CO(21), CO(22) and CO(24) rotate nearly 25° around Ru(2) in order to accommodate themselves to the entrance of the bulky phosphine (see Fig. 2).

The rotation around Ru(2) also induces a rotation around Ru(3) and gives rise to the semi-bridging CO(24) and CO(32) ($Ru(2)-C(24)-O(24)$ $154.1(7)^\circ$ and $Ru(3)-C(32)-O(32)$ $165.4(9)^\circ$). The two $Ru(CO)_3P$ moieties are related to each other by a twisting round the Ru(1)–Ru(3) bond of about 31° . The presence of the two bent semi-bridging COs makes the molecule unsymmetrical and chiral. Some of the other complexes reported in Table 6 show analogous behavior [$L = PPh_3$, $PPh(OMe)_2$] [15,16] or a similar trend [$L = P^iPr_2(C_6H_5Cr(CO)_3)$] [21]; the complexes with $L = P(OMe)_3$ [12] and $L = P(OCH_2CF_3)_3$ [15] show the same type of distortion, yet the disorder observed permits no consideration about the carbonyls. In the complex with $L = P(C_4H_9S)_3$ [17] no distortion occurs owing to the great dimensions of the Ru_3 cluster. The great Ru–Ru distances are probably due to the great bulkiness of the ligands.

We have considered tri- and di-substituted phosphine derivatives of triruthenium dodecacarbonyl reported up to now in the literature in order to verify whether the substitution of phosphines for carbonyls modifies the electronic and steric properties of these clusters, thus making them more or less active in homogeneous catalysis.

The examination of Tables 5 and 6 shows that phosphine ligands are always in equatorial position and that for bi- and trisubstituted derivatives only structures of type 1 are found. Complexes of type 2 occur only when phosphine ligands are bidentate (e.g. dppm). The great variability of Ru–Ru distances even in two molecules in the asymmetric unit does not allow a correlation with

the electronic properties of phosphine ligands and is in keeping with a high degree of flexibility of the metallic cluster. It seems to be more likely that molecular structures are a consequence of a minimization of steric inter- and intramolecular repulsions.

3.4. Catalytic reaction mechanisms

In a previous study on the catalytic activity of phosphine-substituted ruthenium clusters in homogeneous hydrogenation–isomerization of 1,4-pentadiene, we observed that clusters **1** and **2** are considerably active and selective, giving TOF values of 946.5 and 379.5 and selectivities to 1,3-pentadiene of 79.6 and 86.9, respectively. Attempts had been made to correlate the activity to the number and to the pK_a of the phosphines. It has

Table 4

Selected bond lengths (Å) and angles (°) for $\text{Ru}_3(\text{CO})_{10}(\text{PEt}_3)_2$ (complex **3**)

Bond lengths (Å)	
Ru(1)–Ru(2)	2.868(2)
Ru(1)–Ru(3)	2.855(2)
Ru(2)–Ru(3)	2.863(2)
Ru(1)–P(1)	2.343(3)
Ru(3)–P(2)	2.358(3)
Ru(1)–C(11)	1.892(7)
Ru(1)–C(12)	1.957(6)
Ru(1)–C(13)	1.949(7)
Ru(2)–C(21)	1.898(11)
Ru(2)–C(22)	1.967(9)
Ru(2)–C(23)	1.918(7)
Ru(2)···C(32)	2.762(9)
Ru(2)–C(24)	1.976(7)
Ru(3)–C(31)	1.887(8)
Ru(3)–C(32)	1.954(7)
Ru(3)–C(33)	1.950(7)
Ru(3)···C(24)	2.485(9)
C–O av.	1.133(9)
Bond angles (°)	
Ru(1)–Ru(3)–Ru(2)	60.22(6)
Ru(1)–Ru(2)–Ru(3)	59.75(6)
Ru(2)–Ru(1)–Ru(3)	60.03(4)
Ru(2)–C(24)–O(24)	154.1(7)
Ru(3)–C(32)–O(32)	165.4(9)
Ru–C–O av.	176.6(8)
C(11)–Ru(1)–P(1)	94.3(3)
C(12)–Ru(1)–P(1)	92.1(2)
C(13)–Ru(1)–P(1)	91.3(3)
C(11)–Ru(1)–C(12)	94.9(3)
C(11)–Ru(1)–C(13)	96.0(4)
C(21)–Ru(2)–C(22)	98.8(4)
C(21)–Ru(2)–C(23)	99.5(4)
C(21)–Ru(2)–C(24)	93.4(4)
C(22)–Ru(2)–C(23)	91.7(3)
C(23)–Ru(2)–C(24)	91.1(3)
C(31)–Ru(3)–P(2)	95.8(3)
C(32)–Ru(3)–P(2)	92.0(3)
C(33)–Ru(3)–P(2)	90.4(2)
C(31)–Ru(3)–C(32)	92.1(4)
C(31)–Ru(3)–C(33)	92.5(3)

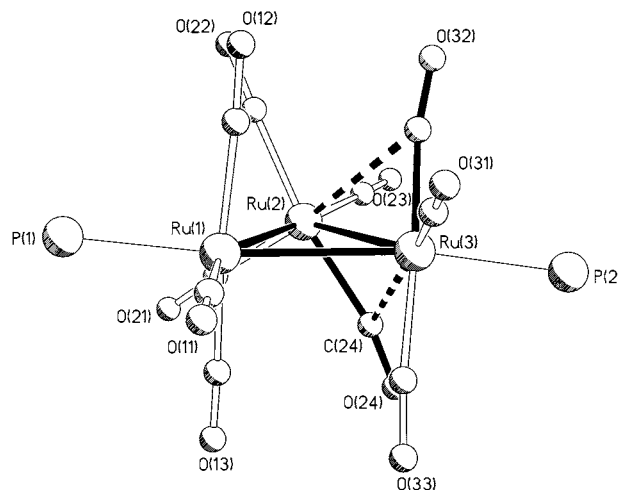


Fig. 2. A diagram of the molecular structure of complex **3** showing the orientations of the carbonyls with respect to the Ru_3 plane.

also been observed that the trisubstituted derivatives are more active than less substituted complexes and that CO does not inhibit the reactions, whereas an excess of free phosphine initially results in lower activities, but gives, after a while, the same results obtained without it [5].

Finally, we found that disproportionation, CO and phosphine displacement and formation of fragments occurred either during the synthesis of complexes **2** and **3** and during catalytic reactions [6]; the same apparently occurred during these catalytic reactions.

In the present work, we have observed that complexes **1**, **2** show good activity in the hydrogenation of diphenylacetylene and that their activity is apparently related to the type of phosphinic substituent (complex **1** is considerably more active than **2**). Moreover complex **3**, formed upon disproportionation during the catalytic reactions of **2**, is also an active catalytic species. A disproportionation and/or fragmentation mechanism can also be inferred from the findings of Bhaduri and coworkers; they found that complex **1** shows a modest catalytic activity in the homogeneous catalytic hydrogenation of cyclohexene [18]; under dihydrogen ‘disproportionation’ occurs leading to $\text{H}_4\text{Ru}_4(\text{CO})_{12-n}(\text{PPh}_3)_n$ derivatives, thus indicating, once again, formation and reassembly of metal fragments. By raising the temperature $\text{Ru}_3(\text{CO})_7(\text{PPh}_2)_2(\text{C}_6\text{H}_4)$ (complex **4**) was obtained; this complex was considered as a catalytic hydrogenation intermediate. These observations do also accord with our recent findings on the catalytic activity of **4** [4]. Interestingly, complex **3** could be the precursor of structures such as **4**. Unfortunately, we did not observe any such complex in our experiments. Their presence would indeed have pointed to the occurrence of cluster catalysis.

The structural parameters of complexes **1** and **2** and of the other phosphine-substituted complexes discussed

above point to a low tendency to release metal fragments and could indicate that formation of cluster **3** could occur only through inter- and intramolecular exchange of phosphines and CO [9] rather than through a dismutation path requiring cluster fragmentation and reassembly of metal fragments. On the other hand, we cannot exclude that the phosphines present on all the ruthenium atoms of such trinuclear derivatives could favor fragmentation by keeping in solution mononuclear fragments. Indeed, it was recently found that phosphine substitution for CO on the metallacyclic cluster $\text{Os}_3(\text{CO})_9(\text{C}_4\text{Ph}_4)$ at room temperature gives monosubstituted products via associative adduct formation only for small phosphines (Tolman's cone angle below 143°). Indeed, bulky phosphines cause fragmentation to mono- and dinuclear products [19]. Finally, the presence of bent semi-bridging carbonyls on complex **2** would favor fragmentation [20].

In conclusion, the observed results (effect of dihydrogen pressure and S/C ratio), the inhibition of the reactions when CO is used, the high catalytic activity of

complex **3** and the 'disproportionation' occurring during the catalytic experiments suggest the possibility that fragmentation occurs together with the formation of some smaller cluster or mononuclear species active in the catalytic cycle. A possible reaction scheme is envisaged in Scheme 1.

Finally, it is worth noting that substitution of SMe_2 for CO at a ruthenium atom of the Ru_3 triangle that contains a bridging C_2Ph_2 ligand in the layer segregated cluster $\text{Pt}_3\text{Ru}_6(\text{CO})_{20}(\text{C}_2\text{Ph}_2)(\mu_3\text{-H})(\mu\text{-H})$ results in a higher activity in the hydrogenation of diphenylacetylene [21]. It was proposed that the enhanced activity could be due to the lability of the SMe_2 ligand, which would easily be displaced, leaving a free coordination site; when this site is occupied again by CO, the activity is reduced to that of the parent cluster. It was also proposed that all catalytic transformations occur at the triruthenium triangle and that platinum exerts a promotional effect by donating electronic density, i.e. a 'metal-to-metal ligand' effect. We have found that an extra CO in place of a phosphine ligand does increase the activity (cluster **3** versus **2**); we suggest that this

Table 5
Structural parameters for $\text{Ru}_3(\text{CO})_9\text{L}_3$ derivatives

L	Ru–Ru (Å)			Type	Tolman's cone angle ($^\circ$)	Ref.
	a	b	c			
CO	2.8595(4)	2.8512(4)	2.8518(4)	1		[11]
PMe_3	2.860(1)	2.862(2)	2.854(1)	1	118	[12]
PMe_2Ph	2.851(1)	2.864(1)	2.860(1)	1	122	[13]
$\text{PMe}_2(\text{CH}_2\text{Ph})$	2.860(2) ^a			1	120	[13]
$\text{P}(\text{OEt})_3$	2.863(1)	2.852(2)	2.851(1)	1	109	[13]
$\text{P}(\text{OMe})_2\text{Ph}$ ^b	2.900(2)	2.870(1)	2.887(2)	1	115	[13]
	2.887(1)	2.894(1)	2.876(2)	1		
	2.884(1)	2.876(1)	2.882(1)	1		
	2.882(4)	2.874(2)	2.885(1)	1		
$\text{P}(\text{OCH}_2\text{CF}_3)$	2.857(2)	2.866(2)	2.852(2)	1	110	[13]
PCy_3	2.9396(8) ^a			1	170	[14]
$\text{P}(\text{OMe})_3$ ^c	2.844(1)	2.849(1)	2.869(1)	1	107	[23]
	2.857(2)	2.853(1)	2.885(2)	1		
AsMe_2Ph ^d	2.851(1)	2.846(1)	2.838(1)	1	120	[13]
	2.846(1)	2.848(1)	2.838(1)	1		

^a The molecule lies on a threefold axis.

^b Four independent molecules.

^c Two polymorphs (triclinic and monoclinic).

^d Two independent molecules.

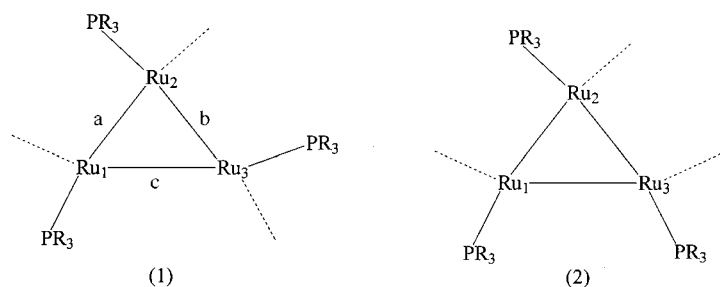


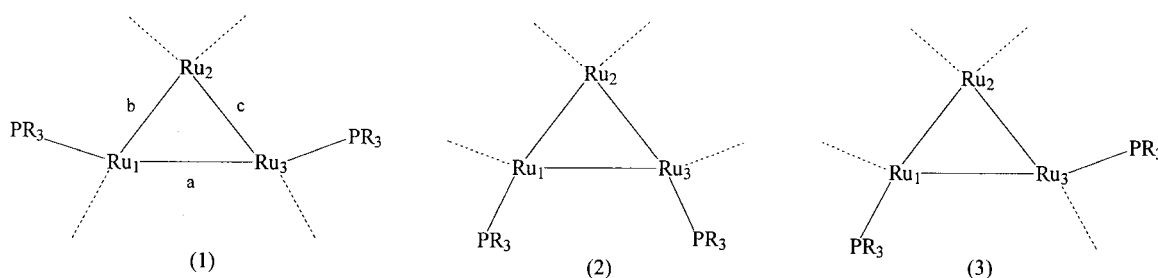
Table 6
Structural parameters for $\text{Ru}_3(\text{CO})_{10}\text{L}_2$ complexes

L	Ru–Ru ^a			Type	Tolman's cone angle	Ref.
	A	b	c			
PPh_3 ^b	2.852(1)	2.833(3)	2.823(3)	1	145°	[16]
	2.893(3)	2.863(3)	2.873(3)	1		
PPh_3 ^b	2.846(3)	2.842(4)	2.838(4)	1	145°	[15]
	2.893(3)	2.873(3)	2.881(3)	1		
PEt_3	2.855(2)	2.868(2)	2.863(2)	1	132°	tw
P(OMe)_3	2.845(1)	2.859(1)	2.845(1)	1	107°	[12]
$\text{P(OMe)}_2\text{Ph}$	2.860(1)	2.865(1)	2.868(1)	1	115°	[15]
$\text{P(OCH}_2\text{CF}_3)_3$	2.831(2)	2.847(2)	2.861(2)	1	110°	[15]
$\text{P(SC}_4\text{H}_9)_3$	2.880(1)	3.003(1)	2.945(1)	1	150°	[17]
$\text{P}^t\text{Pr}[\text{C}_6\text{H}_5\text{Cr(CO)}_3]$	2.8914(8)	2.8927(6) ^c		1	164°	[22]

^a See annexed scheme.

^b Two independent molecules.

^c The molecule lies on a 2-fold axis.



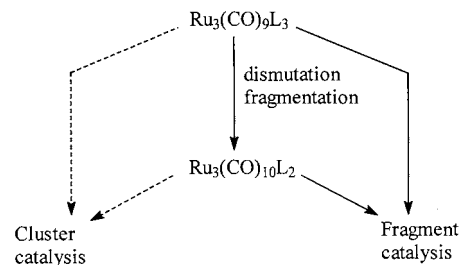
could be due to the better coordinating properties of phosphine ligands with respect to dimethyl sulphide.

In Table 7 the catalytic results observed for clusters 1–3 are compared with those for other ruthenium clusters, unsubstituted and/or substituted with phosphine and phosphido-ligands. The activity observed for clusters 1, 2 and 3 is indeed rather high; only complexes containing benzyne or alkyne ligands show higher activity. It is worth noting that for such derivatives cluster catalysis was observed [4].

In this work we have observed that phosphine-substituted triruthenium clusters are rather active in the hydrogenation of diphenylacetylene: as for structure–reactivity relationships, we have found that the bonding parameters of such clusters cannot be linked to their hydrogenation activity. However, the phosphine substituents may play a role either in determining catalytic activity (cluster catalysis) and in promoting fragmentation of the clusters (fragment catalysis).

4. Supplementary material

Full tables of anisotropic thermal parameters, of hydrogen atomic coordinates, of bond distances and



Scheme 1.

angles are available on request from the Cambridge Crystallographic Data Centre as supplementary publication CCDC No. 117035. Copies of the data can be obtained free of charge on application to: The Director, CCDC, 12 Union Road, Cambridge, CB2 1EZ, UK (Fax: +44-1223-336-033; email: deposit@ccdc.cam.ac.uk or www: <http://www.ccdc.cam.ac.uk>).

Acknowledgements

Support for this work has been obtained from MURST (Italy) under the form of a cofinancing pro-

Table 7

Comparison between the catalytic activities of clusters 1–3 and those of other ruthenium-based trinuclear complexes — hydrogenation of diphenylacetylene

Cluster ^a	S/C ratio	TOF ^b	Selectivity ^c	Reference
A	49.4	97.4	100	[6]
B	60.3	117.3	100	[6]
C	100.0	99.1	99.3	[6]
D	108.0	90.1	100	[6]
Cluster 1	761.1	155.9	93.0	this work
Cluster 2	153.3	119.5	99.3	this work
Cluster 3	278.9	193.9	99.6	this work
E	194.6	700.8	98.7	[6]
F	559.2	250.8	81.1	[6]

^a (A) Ru₃(CO)₁₂. (B) H₄Ru₄(CO)₁₂. (C) HRu₃(CO)₉(PPh₂). (D) HRu₃(CO)₇(PPh₂)₃. (E) Ru₃(CO)₇(PPh₂)₂(C₆H₄). (F) Ru₃(CO)₇(PPh₂)₂(HC₂Ph).

^b TOF = Turnover frequency (TON h⁻¹).

^c To monoenes.

gram between the Università di Torino and the Università del Piemonte Orientale (Alessandria).

References

- [1] R. Giordano, E. Sappa, J. Organomet. Chem. 448 (1993) 157.
- [2] M. Castiglioni, R. Giordano, E. Sappa, J. Organomet. Chem. 491 (1995) 111.
- [3] (a) D. Cauzzi, R. Giordano, E. Sappa, A. Tiripicchio, M. Tiripicchio Camellini, J. Clust. Sci. 4 (1993) 279. (b) R. Giordano, E. Sappa, S.A.R. Knox, J. Cluster Sci. 7 (1996) 263.
- [4] M. Castiglioni, S. Deabate, R. Giordano, P.J. King, S.A.R. Knox, E. Sappa, J. Organomet. Chem. 571 (1998) 251.
- [5] M. Castiglioni, R. Giordano, E. Sappa, J. Organomet. Chem. 342 (1988) 111.
- [6] M. Castiglioni, R. Giordano, E. Sappa, J. Organomet. Chem. 342 (1988) 97.
- [7] A.C.T. North, D.C. Phillips, F.S. Mathews, Acta Crystallogr. A 24 (1968) 351.
- [8] H.D. Flack, Acta Crystallogr. A 39 (1983) 876.
- [9] (a) M.I. Bruce, J.G. Matison, B.K. Nicholson, J. Organomet. Chem. 247 (1983) 321. (b) M.I. Bruce, Coord. Chem. Rev. 76 (1987) 1.
- [10] A. Poe, Chem. Br. (1983) 997.
- [11] M.R. Churchill, F.J. Hollander, J.P. Hutchinson, Inorg. Chem. 16 (1977) 2655.
- [12] M.I. Bruce, J.G. Matison, B.W. Skelton, A.H. White, J. Chem. Soc. Dalton Trans. (1983) 2375.
- [13] M.I. Bruce, M.J. Liddell, O. Bin Shawkataly, C.A. Hughes, B.W. Skelton, A.H. White, J. Organomet. Chem. 347 (1988) 207.
- [14] G. Suss-Fink, J. Godefroy, V. Ferrand, A. Neels, H. Stoeckli-Evans, J. Chem. Soc. Dalton Trans. (1998) 515.
- [15] M.I. Bruce, M.J. Liddell, C.A. Hughes, J.M. Patrick, B.W. Skelton, A.H. White, J. Organomet. Chem. 347 (1988) 181.
- [16] T. Chin-Choy, N.L. Kader, G.D. Stucky, P.C. Fors, J. Organomet. Chem. 346 (1988) 225.
- [17] U. Bodensieck, H. Vahrenkamp, G. Rheinwald, H. Stoeckli-Evans, J. Organomet. Chem. 488 (1995) 85.
- [18] A. Basu, S. Bhaduri, H. Khwaja, P.G. Jones, T. Schroeder, G.M. Sheldrick, J. Organomet. Chem. 290 (1985) C19.
- [19] A.J. Poe, D.H. Farrar, R. Ramachandran, C. Moreno, Inorg. Chim. Acta 274 (1998) 82.
- [20] C.Q. Simpson II, M.B. Hall, J. Am. Chem. Soc. 114 (1992) 1641.
- [21] R.D. Adams, T.S. Barnard, Organometallics 17 (1998) 2885.
- [22] R. Cullen, S.J. Rettig, H. Zhang, Can. J. Chem. 74 (1996) 2167.
- [23] L.J. Farrugia, C. Rosenhahn, S. Whitworth, J. Cluster Sci. 9 (1998) 505.